The American Journal of Pathology, Vol. 169, No. 4, October 2006

DOI: 10.2353/ajpath.2006.051136

Gastrointestinal, Hepatobiliary and Pancreatic Pathology

Inhibition of Intrahepatic Bile Duct Dilation of the Polycystic Kidney Rat with a Novel Tyrosine Kinase Inhibitor Gefitinib

Yasunori Sato,* Kenichi Harada,* Shinichi Furubo,† Kazuo Kizawa,† Takahiro Sanzen,† Mitsue Yasoshima,* Satoru Ozaki,* Kumiko Isse,* Motoko Sasaki,* and Yasuni Nakanuma*

From the Department of Human Pathology, Kanazawa University Graduate School of Medicine, Kanazawa; and the Drug Safety Research Laboratory,† Toyama Chemical Company Limited, Toyama, Japan*

The polycystic kidney (PCK) rat represents a liver and kidney cyst pathology corresponding to Caroli's disease with congenital hepatic fibrosis and autosomal recessive polycystic kidney disease. We previously reported that an epidermal growth factor receptor tyrosine kinase inhibitor, gefitinib (Iressa), significantly inhibited the abnormal growth of biliary epithelial cells of PCK rats *in vitro*. This study investigated the effects of gefitinib on cyst pathogenesis of the PCK rat both *in vitro* and *in vivo*. A three-dimensional culture model of biliary epithelial cells in the collagen gel matrix was used for *in vitro* analysis. For *in vivo* experiments, PCK and control rats were treated with gefitinib between 3 and 10 weeks of age. *In vitro*, gefitinib had strong inhibitory effects on biliary cyst formation of PCK rats. *In vivo*, treatment with gefitinib significantly inhibited the cystic dilatation of the intrahepatic bile ducts of PCK rats, which was accompanied by improvement of liver fibrosis. By contrast, no beneficial effects were observed on renal cyst development because of the treatment. These results suggest that signaling pathways mediated by epidermal growth factor receptor are involved in biliary dysgenesis of the PCK rat, with the mechanisms of cyst progression being different between the liver and kidney. *(Am J Pathol 2006, 169:1238–1250; DOI: 10.2353/ajpath.2006.051136)*

The polycystic kidney (PCK) rat, an animal model of human autosomal recessive polycystic kidney disease (ARPKD), represents a liver fibrocystic pathology corresponding to Caroli's disease with congenital hepatic fibrosis.[1,2] ARPKD is a form of inherited childhood nephropathy, with an incidence of 1 in 20,000 live births.[3,4] The disease is characterized by the fusiform dilatation of collecting tubules and by biliary dysgenesis and hepatic fibrosis. Fetal or neonatal death is often caused, owing to tremendous bilateral enlargement of the kidneys, impaired lung formation, and pulmonary hypoplasia. Progression to end-stage renal disease occurs in 20 to 45% of cases within 15 years. A proportion of the patients maintain renal function into adulthood, when complications of liver disease predominate.[4]

The liver and kidney lesions in ARPKD patients and in PCK rats are caused by mutations to orthologous genes, *PKHD1/Pkhd1*.[5,6] *PKHD1* is a large gene from which multiple transcripts may be generated by alternative splicing.[4,7] In common with other PKD-related proteins, the ARPKD protein fibrocystin is localized to the primary cilia of renal epithelial cells and is often absent in ARPKD tissue.[8–10] In intrahepatic bile ducts of normal rats, each cholangiocyte has a single cilium that expresses fibrocystin, whereas the cilia of PCK rats show an abnormal morphology devoid of fibrocystin.[11,12] The link between cyst development and ciliary dysfunction attributable to the lack of fibrocystin has been suggested, although the precise role of fibrocystin in cyst development remains unclear.[13]

It has been well established that the epidermal growth factor (EGF)/transforming growth factor (TGF)-α/EGF receptor (EGFR) pathway and the adenosine 3′,5′-cyclic monophosphate (cAMP) pathway play important roles in promoting the renal tubular epithelial cell proliferation and cyst formation in ARPKD as well as in the autosomal dominant form of PKD (ADPKD).[14–19] Consequently, a number of studies have examined the effects of blocking these pathways in animal models of PKD. For example, inhibition of the EGFR tyrosine kinase activity inhibited renal cyst development in bpk and orpk mice (models of

Accepted for publication July 11, 2006.

Address reprint requests to Yasuni Nakanuma, M.D., Ph.D., Department of Human Pathology, Kanazawa University, Graduate School of Medicine, Kanazawa 920-8640. E-mail: pbcpsc@kenroku.kanazawa-u.ac.jp.

ARPKD) and in Han:SPRD rat (a model of ADPKD).[15,20–22] The administration of a vasopressin V2 receptor (VPV2R) antagonist lowered the renal cAMP level, and inhibited renal cystogenesis in pcy mouse (a model of nephronophthisis) and in *Pkd2*$^{-/tm1Som}$ mouse (a model of ADPKD).[23,24] Recently, it has been shown that that the VPV2R antagonist improved the renal disease development and progression of the PCK rat.[25] In these studies, however, the VPV2R antagonist did not improve the fibrocystic liver disease of the PCK rat. Inhibition of PKD of the PCK rat by the use of EGFR tyrosine kinase inhibitors (EKI-785 and EKB-569) resulted in no effect or a worsened PKD as well as no significant effect on the fibrocystic liver disease.[26]

EGFR tyrosine kinase activation triggers numerous downstream signaling pathways, such as the extracellular-regulated protein kinase (ERK)/mitogen-activated protein kinase (MAPK), and the phosphoinositide-3-kinase (PI3K)/Akt pathways.[27] Recently, we demonstrated that biliary epithelial cells (BECs) isolated from the PCK rat were hyperreactive to EGF, which was accompanied by the activation of the MAPK pathway consisting of MAPK/ERK kinase 5 (MEK5)/ERK5 *in vitro*.[28] We also showed that an EGF tyrosine kinase inhibitor, gefitinib (Iressa), significantly inhibited the abnormal growth of cultured BECs of the PCK rat.

The PCK rat is regarded as a slowly progressive model of ARPKD. Therapies for liver lesions of ARPKD are particularly important because liver disease becomes a major cause of morbidity and mortality in elderly patients of ARPKD.[4] To date, there has been no study that has successfully inhibited the fibrocystic liver disease of the PCK rat. This study aimed to inhibit the cystic dilation of the intrahepatic bile ducts and hepatic fibrosis as well as the PKD of the PCK rat by the use of a novel tyrosine kinase inhibitor gefitinib.

Materials and Methods

Animals

PCK rats were maintained at the Laboratory Animal Institute of Kanazawa University Graduate School of Medicine. Control (Sprague-Dawley) rats were purchased from Charles River Japan (Sagamihara, Japan). The rats were maintained on a standard laboratory rat diet and water *ad libitum*. All studies were performed in accordance with the Guidelines for the Care and Use of Laboratory Animals at Takara-machi Campus of Kanazawa University, Kanazawa, Japan.

Three-Dimensional Cell Culture in Collagen Gel Matrix

Intrahepatic BECs were isolated, purified, and cultured from 8-week-old rats as described previously.[28] Because the dilatation of the intrahepatic large bile ducts has been regarded as an essential feature of Caroli's disease, BECs were isolated from intrahepatic large bile ducts. The fourth subcultured BECs were used for the study. A three-dimensional cell culture in a collagen gel matrix was performed according to the previously described method with some modifications.[29] In brief, BECs were dispersed and directly embedded in a fluid collagen gel matrix (Cellmatrix Type 1-A; Nitta Gelatin, Osaka, Japan). The collagen gel matrix was composed of 0.3% Cellmatrix Type 1-A, 10× concentrated Dulbecco's modified Eagle's medium and nutrient mixture F-12 (1:1; Life Technologies, Inc., Rockville, MD) containing an 8:1:1 ratio of 0.05 N sodium hydroxide, 260 mmol/L sodium bicarbonate, and 200 mmol/L HEPES. The cellular density at the beginning of the culture was 1×10^5 cells/ml. The fluid collagen gel was planted on six-well plates. This collagen fluid soon became gelatinous. The cultures were then covered with a culture medium composed of Dulbecco's modified Eagle's medium and nutrient mixture F-12 (Life Technologies, Inc.), 10% Nu-Serum (Becton Dickinson, Bedford, MA), 1% ITS+ (Becton Dickinson), 5 μmol/L forskolin (Wako Pure Chemical, Osaka, Japan), 12.5 mg/ml bovine pituitary extract (Kurabo Industries, Osaka, Japan), 1 μmol/L dexamethasone (Sigma, St. Louis, MO), 5 μmol/L triiodo-thyronine (Sigma), 5 mg/ml glucose (Sigma), 25 mmol/L sodium bicarbonate (Sigma), 1% antibiotics-antimycotic (Life Technologies, Inc.), and 20 ng/ml EGF (Upstate Biotechnology, Lake Placid, NY) at 37°C in an atmosphere of 5% CO_2. The basal culture medium was changed every 2 days.

Effects of Gefitinib on Biliary Cyst Formation in Vitro

The effects of gefitinib on biliary cyst formation were examined using the three-dimensional cell culture system. On day 7 after the beginning of cell culture, the culture medium was changed to that containing 20 ng/ml EGF and 0.1, 0.5, or 1 μmol/L gefitinib (Iressa, ZD1839; provided by AstraZeneca, Macclesfield, UK). Incubation was continued for a further 12 days. The culture medium was changed every 2 days. The cultured cells were observed daily under phase-contrast microscopy (Olympus, Tokyo, Japan), and their morphological changes were recorded using a digital camera (model DXC-S500; Sony, Tokyo, Japan). The recorded images were reproduced on a computer, and cyst size was determined using image analysis software (Win ROOF version 3.6; Mitani Corp., Tokyo, Japan). Measurement was performed for 10 well-developed cysts for each time after gefitinib treatment, and the mean was calculated. The number of cysts was counted under phase-contrast microscopy at ×40 magnification, and the total cyst number of five fields was determined at each time.

To determine whether gefitinib can prevent biliary cyst formation when it is administrated before BECs start to undergo cyst formation, 0.1 or 1 μmol/L gefitinib was administrated at the beginning of the three-dimensional cell culture in the presence of 20 ng/ml EGF. The culture medium was changed every 2 days. For 12 days after starting the treatment, the number and size of the cysts were determined as above.

Apoptosis Assay

The effect of gefitinib on apoptosis of cultured BECs was determined using the single-stranded DNA (ssDNA) apoptosis enzyme-linked immunosorbent assay kit (Chemicon Int., Temecula, CA) according to the manufacturer's instructions. This method is based on the selective denaturation of DNA in apoptotic cells by formamide, which is a gentle agent that denatures DNA in apoptotic cells, but not in necrotic cells or in cells with DNA breaks in the absence of apoptosis.[30] In brief, a total of 1250 cells per well were seeded in a 96-well collagen-coated plate. After a 48-hour preincubation with the basal medium, the medium was exchanged for that containing appropriate concentrations of gefitinib and incubated at 37°C in an atmosphere of 5% CO_2 for a further 24 or 72 hours. The cells were fixed with 80% methanol in phosphate-buffered saline (PBS) on the wells and incubated with formamide at 75°C for 20 minutes. For negative control wells, S1 nuclease (10 U/well) (Takara Bio, Otsu, Japan) was added and incubated at 37°C for 30 minutes for the removal of single-stranded regions in DNA-DNA hybrids. After washing with PBS, the wells were incubated with 2.5% bovine serum albumin at 37°C for 1 hour to block nonspecific binding sites and then incubated with antibody mixture (primary monoclonal to ssDNA and horseradish peroxidase-labeled anti-mouse IgM; provided in the kit) at room temperature for 30 minutes. After washing, color development was performed with 2,2′-azinobis(3-ethylbenziazoline-6-sulfoic acid) solution, and its absorbance at 405 nm was measured using a microplate reader.

As an additional experiment, DNA fragmentation attributable to apoptosis was detected using a terminal dUTP nick-end labeling (TUNEL) method. Three-dimensional cell culture in collagen gel matrix was performed as above. On day 7 after the beginning of cell culture, the culture medium was changed for those containing appropriate concentrations of gefitinib. The culture medium was changed every 2 days. On days 0, 4, 8, and 12 after gefitinib treatment, formalin-fixed, paraffin-embedded sections (4 μm thick) of the collagen gel matrix were prepared. After proteinase K digestion and endogenous peroxidase blocking, the sections were stained by using a commercial kit (TdT-FragEL DNA fragmentation detection kit; Calbiochem, San Diego, CA). After color development with 3,3′-diaminobenzidine tetrahydrochloride, sections were counterstained with methyl green.

In Vivo *Administration of Gefitinib*

A total of 30 male rats were used. At 3 weeks of age, 15 normal and 15 PCK rats were divided into one control and two experimental groups. The experimental groups (five rats per group) were intraperitoneally administered 2 or 10 mg/kg gefitinib daily between 3 and 10 weeks of age. The dosage was determined based on our preliminary experimental data, as well as the recommendation of the AstraZeneca group of companies. The control group received vehicle (2% Tween 80 and 0.5% methylcellulose in water) alone.

At 10 weeks of age, rats were weighed and anesthetized with diethylether. Blood was obtained by cardiac puncture for the determination of serum levels of aspartate aminotransferase, alanine aminotransferase, alkaline phosphatase, total protein, albumin, blood urea nitrogen, and creatinine. The liver and kidney were weighed and immersed in 10% formalin neutral buffer solution (pH 7.4), and the tissues were embedded in paraffin for histological analysis. Parts of the tissues were immediately frozen in liquid nitrogen to use for Western blot analysis, the reverse transcriptase-polymerase chain reaction (RT-PCR), and collagen content measurement.

Silicon Rubber Cast Study

The three-dimensional observation of the intrahepatic biliary tree was performed using a silicon rubber cast study as previously described.[2] In brief, a cannula was inserted into the extrahepatic bile duct, and Microfil compound (MV-112; Flow Tech. Inc., Carver, MA) was injected using a syringe. The Microfil compound-injected liver specimens were placed in a refrigerator at 4°C overnight to allow polymerization. Then they were immersed in 25% ethanol for 24 hours. At 24-hour intervals, the ethanol concentration was raised to 50, 75, 95, and 100%. Finally, the specimens were immersed in methyl salicylate for the cleaning of the tissue.

RT-PCR

Total RNA (1 μg) was extracted from the liver using an RNA extraction kit (RNeasy Mini; Qiagen, Tokyo, Japan) and was used to synthesize cDNA with reverse transcriptase (ReverTra Ace; Toyobo Co., Osaka, Japan). PCR amplification was performed in a total volume of 25 μl containing 1 μl of cDNA, 0.2 mmol/L dNTPs, 1 μmol/L each of 5′- and 3′-primers, and 2.5 U of *Taq*DNA polymerase (Takara EX *Taq*; Takara Bio) with an annealing temperature of 60°C. The sequences of the rat primers were as follows: connective tissue growth factor (CTGF), 5′-GAAAGACAGGTACTAGCTGA-3′ (forward) and 5′-GAACAATAGGCACAAACGTC-3′; TGF-β1, 5′-CAATTCCTGGCGTTACCTTG-3′ (forward) and 5′-GAAGCAGTAGTTGGTATCCA-3′ (reverse); and β-actin, 5′-ACCTTCAACACCCCAGCCATGTAC-G-3′ (forward) and 5′-CTGATCCACATCTGCTGGAAG-GTGG-3′ (reverse). The number of PCR cycles for CTGF, TGF-β1, and β-actin were 30, 35, and 25, respectively. For each reaction, an initial denaturation cycle of 94°C for 3 minutes and a final cycle of 72°C for 10 minutes were incorporated. The PCR products were subjected to 2% agarose gel electrophoresis and stained with ethidium bromide. Semiquantitative analysis of the gel image was performed using the public domain NIH Image software in the exponential range of each PCR amplification. The fold difference compared with β-actin expression was calculated.

Immunohistochemistry

Formalin-fixed, paraffin-embedded sections (4 μm thick) were deparaffinized. Antigen retrieval was performed for the antibodies against phosphorylated (p-)ERK1/2, p-ERK5, cytokeratin, and Ki-67 protein by microwaving in 10 mmol/L citrate buffer (pH 6.0). After blocking of the endogenous peroxidase, the sections were incubated overnight at 4°C with individual primary antibodies: anti-p-ERK1/2 (1:200) (44-680, rabbit polyclonal; Biosource Int., Camarillo, CA), anti-p-ERK5 (1:100) (KAS-MA002, rabbit polyclonal; Stressgen, San Diego, CA), anti-cytokeratin (1:600) (A0575, rabbit polyclonal; DAKO, Glostrup, Denmark), anti-ssDNA (1:400) (A4506, rabbit polyclonal; DAKO), and anti-Ki-67 protein (1:50) (MIB-5, mouse monoclonal; Immunotech, Marseille, France). Then the sections were incubated with secondary antibody conjugated to the peroxidase-labeled polymer, EnVison+ system (DAKO). Color development was performed using 3,3′-diaminobenzidine tetrahydrochloride, and the sections were counterstained with hematoxylin. Control sections were evaluated by substitution of the primary antibodies with nonimmunized serum, resulting in no signal detection.

Histological Assessment

Formalin-fixed, paraffin-embedded sections were prepared for the liver and kidney, and whole tissue sections were used to measure cyst volumes and liver fibrosis. Cyst volumes of the liver and kidney were assessed using immunostained sections with anti-cytokeratin antibody and hematoxylin and eosin (H&E) staining of sections, respectively. Liver fibrosis was assessed using picrosirius red staining. Stained sections were visualized under an Olympus light microscope, and the digital images were acquired and reproduced on a computer using the image processing software Viewfinder Lite (version 1.0; Pixera Corp., Los Gatos, CA). Image analysis was performed in software using Win ROOF (Mitani Corporation). A color threshold was applied at a level that separated cysts from noncystic tissue or the picrosirius red-stained material from the background to calculate the volume of the cysts or fibrosis. The areas of interest were expressed as a percentage of the total tissue.

Evaluation of apoptosis was performed using sections stained using the TUNEL method. Liver sections and sections of three-dimensional cell culture of BECs were used for the analysis. More than 500 BECs and hepatocytes were surveyed in liver sections, and more than 200 BECs for each section of collagen gel matrix were surveyed. The percentage of BECs positive for TUNEL was expressed as the TUNEL-labeling index (LI). To evaluate the cell proliferative activity, Ki-67 protein-positive signals were similarly counted for BECs of the Ki-67-immunostained liver sections and sections of collagen gel matrix. The percentage of BECs positive for Ki-67 protein was expressed as the Ki-67-LI.

Western Blot Analysis

Proteins were extracted from the liver specimens and cultured BECs using T-PER tissue protein extraction reagent (Pierce Chemical Co., Rockford, IL), and the total protein was measured spectrometrically. First, 100 μg of the protein was subjected to 10% SDS-polyacrylamide electrophoresis and then electrophoretically transferred onto a nitrocellulose membrane. The membrane was incubated with primary antibodies against EGFR (1:100) (sc-03, rabbit polyclonal; Santa Cruz Biotechnology, Santa Cruz, CA), p-EGFR (1:100) (sc-12351, rabbit polyclonal; Santa Cruz Biotechnology), p-ERK1/2 (1:100) (Biosource International), p-ERK5 (1:400) (Stressgen), and actin (1:100) (sc-10731, rabbit polyclonal; Santa Cruz Biotechnology). The protein expression was detected using an EnVison+ system (DAKO). 3,3′-Diaminobenzidine tetrahydrochloride was used as the chromogen.

Measurement of Collagen Content

Liver specimens (40 to 60 mg, wet weight) were homogenized with T-PER tissue protein extraction reagent (Pierce Chemical Co.). Homogenates were centrifuged and filtered through a 0.22-μm sterile filter. The collagen content of the specimens was measured using the Sircol collagen assay kit (Biocolor Ltd., Belfast, UK) according to the manufacturer's instructions. In brief, Sirius red reagent (50 μl) was added to each liver homogenate (50 μl) and mixed for 30 minutes. The collagen-dye complex was precipitated by centrifugation at 15,000 × *g* for 5 minutes, washed with ethanol, and dissolved in 0.5 mol/L sodium hydroxide. Finally, the samples were introduced into a microplate reader, and the absorbance was determined at 540 nm.

Satatistics

The mean ± SD was calculated for all parameters. Statistical differences were determined using the Mann-Whitney *U*-test or analysis of variance. A P value <0.05 was accepted as the level of statistical significance.

Results

Effects of Gefitinib on Biliary Cyst Formation in Vitro

The three-dimensional cell culture system was used for the determination of the effects of gefitinib on biliary cyst formation. When BECs were cultured in collagen gel matrix with the medium that did not contain gefitinib, the cells became spherical or elliptical small cystic masses 2 to 3 days later as observed under phase-contrast microscopy (Figure 1, A and D). The microcysts gradually enlarged and transformed to multicellular cysts forming well-developed cysts (Figure 1, B and E). The size and number of the biliary cysts increased throughout a period

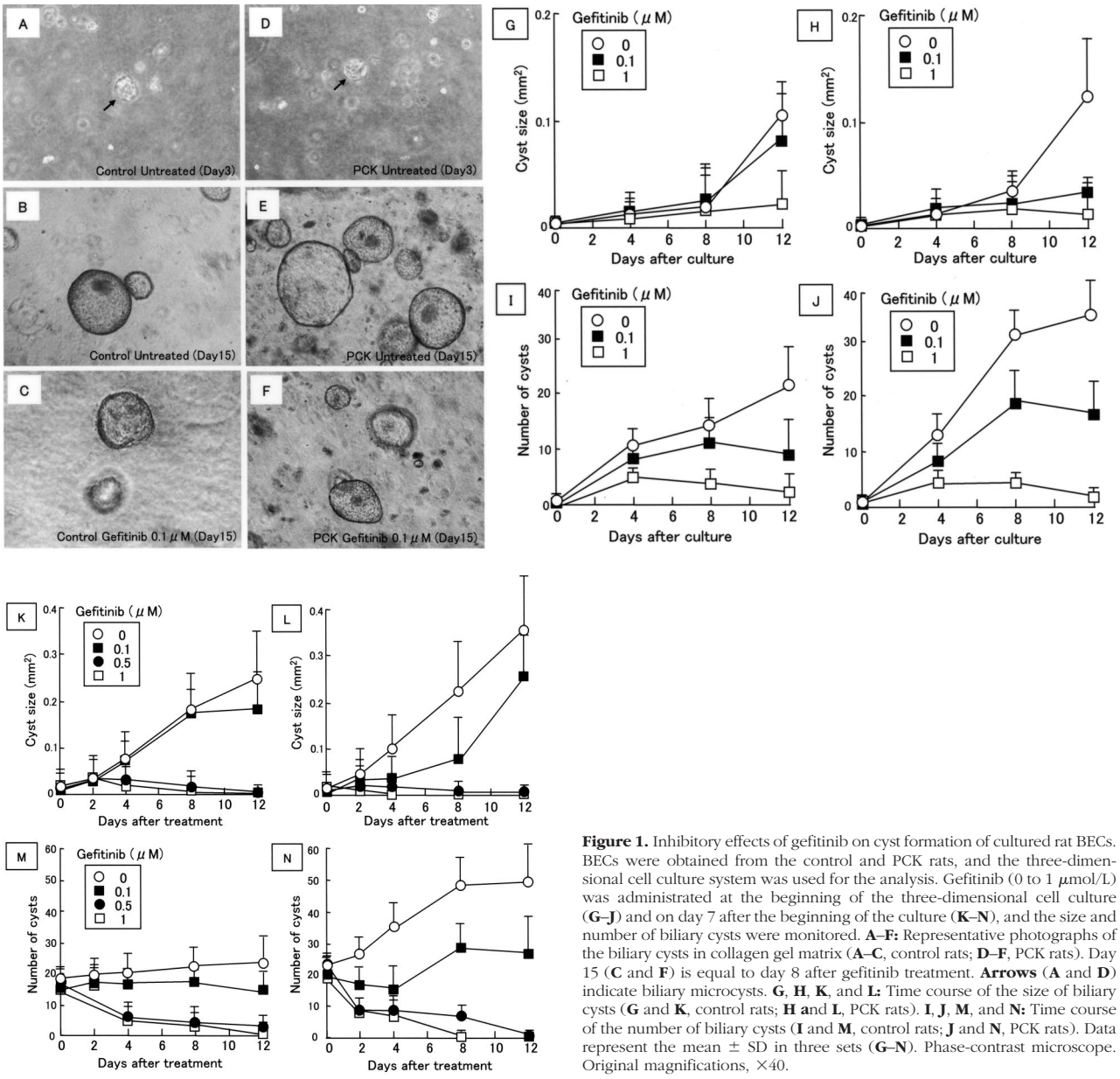

Figure 1. Inhibitory effects of gefitinib on cyst formation of cultured rat BECs. BECs were obtained from the control and PCK rats, and the three-dimensional cell culture system was used for the analysis. Gefitinib (0 to 1 μmol/L) was administrated at the beginning of the three-dimensional cell culture (**G–J**) and on day 7 after the beginning of the culture (**K–N**), and the size and number of biliary cysts were monitored. **A–F:** Representative photographs of the biliary cysts in collagen gel matrix (**A–C**, control rats; **D–F**, PCK rats). Day 15 (**C** and **F**) is equal to day 8 after gefitinib treatment. **Arrows** (**A** and **D**) indicate biliary microcysts. **G**, **H**, **K**, and **L:** Time course of the size of biliary cysts (**G** and **K**, control rats; **H** and **L**, PCK rats). **I**, **J**, **M**, and **N:** Time course of the number of biliary cysts (**I** and **M**, control rats; **J** and **N**, PCK rats). Data represent the mean ± SD in three sets (**G–N**). Phase-contrast microscope. Original magnifications, ×40.

of 2 weeks. Gefitinib was administrated at the beginning of the three-dimensional cell culture, and the size and number of biliary cysts were temporally monitored. Biliary cysts were developed in the control and PCK rats, and gefitinib had dose-dependent inhibitory effects on the size and number of the cysts for both the control and PCK rats (Figure 1, G–J).

When gefitinib was administrated 7 days after the beginning of the three-dimensional cell culture, it also inhibited the increase in the size and number of the cysts for both the control and PCK rats (Figure 1, K–N). The dosage of 0.1 μmol/L gefitinib inhibited cyst formation, which was more prominent in PCK rats than those of control rats, particularly on days 4 and 8 after treatment. At the dosages of 0.5 and 1 μmol/L, once formed, the biliary cysts decreased in size and number and almost disappeared by day 12 after treatment in both the control and PCK rats. Representative photographs of the biliary cysts in the collagen gel matrix are shown in Figure 1, A–F.

Effect of Gefitinib on BEC Apoptosis and Cell Proliferative Activity in Vitro

The cultured BECs were treated with gefitinib for 1 or 3 days and were subsequently subjected to the apoptosis enzyme-linked immunosorbent assay assay. As shown in Figure 2A, apoptotic cell death was detected similarly in the control and PCK rats without gefitinib treatment, and gefitinib had no effect on this basal apoptosis level on day 1. On day 3, gefitinib induced apoptosis of the BECs in both the control and PCK rats in a dose-dependent manner (Figure 2B).

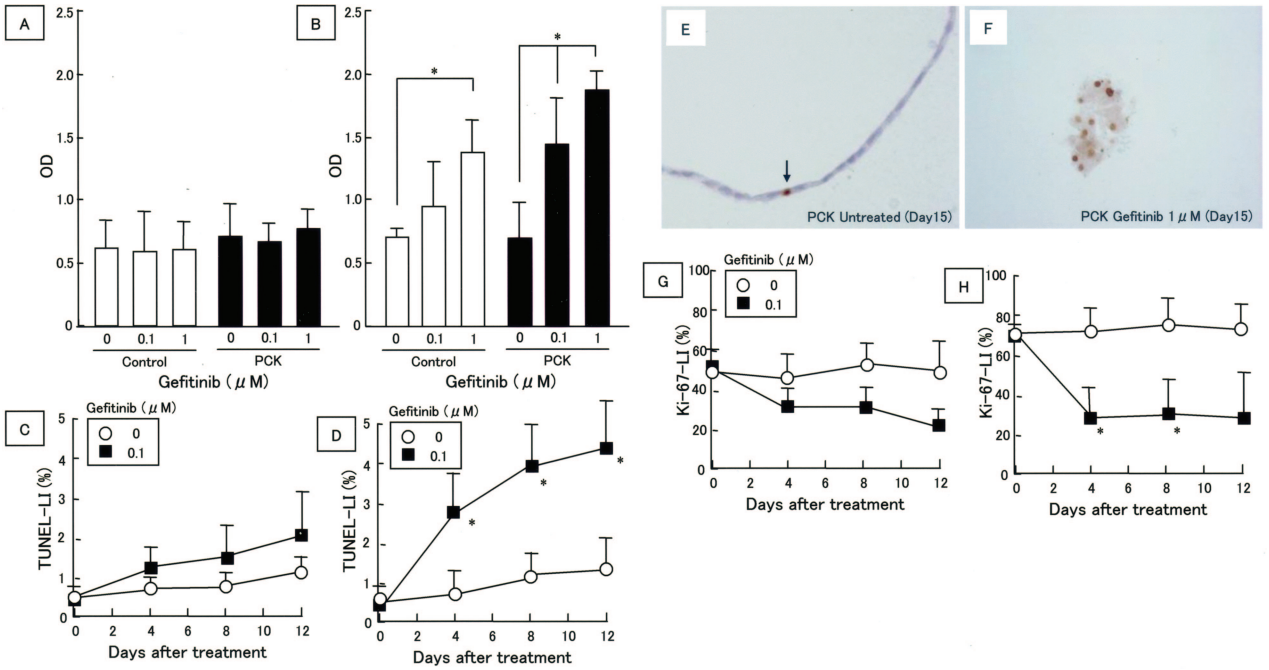

Figure 2. Induction of apoptosis and inhibition of cell proliferative activity in cultured rat BECs by gefitinib. **A** and **B:** Apoptosis was determined using the ssDNA apoptosis enzyme-linked immunosorbent assay kit on day 1 (**A**) and day 3 (**B**) after gefitinib treatment (0 to 1 μmol/L). **C** and **D:** BEC apoptosis determined by the TUNEL method. The TUNEL-labeling index (LI) was determined in sections of collagen gel matrix of the three-dimensional cell culture as described in Materials and Methods (**C**, control rats; **D**, PCK rats). **E** and **F:** Immunostaining using anti-ssDNA antibody. Sections of collagen gel matrix of the three-dimensional cell culture were used. A few nuclei of biliary cysts were labeled with the anti-ssDNA antibody in PCK rats without gefitinib treatment (**E**, **arrow**), whereas many positive nuclear signals were observed with the disintegration of cyst morphology in the PCK rats treated with gefitinib on day 15 (day 8 after gefitinib treatment) (1 μmol/L) (**F**). **G** and **H:** Proliferative activity of BECs. The Ki-67-LI was determined in sections of collagen gel matrix of the three-dimensional cell culture as described in Materials and Methods (**G**, control rats; **H**, PCK rats). Data represent the mean ± SD in six sets (**A** and **B**) and three sets (**C**, **D**, **G**, and **H**). $*P < 0.01$. Original magnifications, ×400.

BEC apoptosis was temporally monitored for days 0 to 12 after gefitinib treatment. The three-dimensional cell culture system and the TUNEL method were used for the analysis. As shown in Figure 2, C and D, the rate of BEC apoptosis was gradually increased up to day 12 after treatment in the control and PCK rats. The mean apoptosis rate was higher in the BECs of PCK rats than in those in control rats on days 4, 8, and 12 after the treatment. The increase in the ratio of gefitinib-induced apoptosis to the untreated status was compared between the control and PCK rats, and the PCK cells showed a significantly increased ratio of apoptosis than the controls on days 4, 8, and 12 after the treatment.

Immunostaining of ssDNA for paraffin-embedded sections of the collagen gel matrix of the three-dimensional cell culture showed that without gefitinib treatment only a few nuclei of the biliary cysts were labeled with the anti-ssDNA antibody in the control and PCK rats (Figure 2E, arrow). Treatment with gefitinib increased the number of ssDNA-positive nuclei of the biliary cysts, and at a high concentration (1 μmol/L) disintegration of the cyst morphology and detachment of cell-to-cell contact were observed with a high incidence of ssDNA-positive nuclear labeling (Figure 2F).

The proliferative activity of the BECs was determined by Ki-67-immunostained sections of the collagen gel matrix. In the absence of gefitinib, the proliferative activity of the BECs was maintained during the course of experiments, and the BECs of PCK rats showed a significantly high cell proliferative activity compared with that of the controls (Figure 2, G and H). Gefitinib reduced the proliferative activity of the BECs of the control and PCK rats, which contrasted with the gradually increasing apoptosis rate of BECs during the course of gefitinib treatment (Figure 2, C and D). When the ratio of the cell proliferative activity of gefitinib-treated cells to the untreated status was compared between the control and PCK rats, there was a statistically significant difference on days 4 and 8 after the treatment (Figure 2H).

In Vivo *Administration of Gefitinib*

Both control and PCK rats were intraperitoneally administrated gefitinib at 2 or 10 mg/kg daily for 7 weeks starting at 3 weeks of age. No significant reduction of the total body weight was observed at these dosages (Table 1). Figure 3 shows morphological changes of the liver and kidney after the treatment.

Livers

Dilated intrahepatic bile ducts were spread in almost all portal areas and were surrounded by portal connective tissue in PCK rats without treatment (Figure 3C). Gefitinib (2, 10 mg/kg) reduced the extent of the dilatation of intrahepatic bile ducts of PCK rats, but the effects appeared to be incomplete, even at a dosage of 10 mg/kg,

Table 1. Treatment of Control and PCK Rats with Gefitinib

	Control	Control	PCK	PCK	PCK
Gefitinib (mg/kg)	0	10	0	2	10
Body weight (g)	344 ± 16	334 ± 16	321 ± 7	308 ± 11	310 ± 5
Liver/body weight (%)	4.1 ± 0.3	3.7 ± 0.4	4.1 ± 0.1	4.5 ± 0.7	4.3 ± 0.1
Kidney/body weight (%)	0.35 ± 0.01	0.33 ± 0.02	0.99 ± 0.10**	1.0 ± 0.20	1.0 ± 0.12
Liver cyst index (%)	ND	ND	7.9 ± 2.7	6.7 ± 1.6	4.1 ± 1.3*
Kidney cyst index (%)	ND	ND	23 ± 2	23 ± 7	27 ± 7
Ki-67-labeling index (%) (bile duct)	0.51 ± 0.22	0.39 ± 0.21	7.9 ± 2.3**	5.8 ± 3.1	3.5 ± 2.1*
TUNEL-labeling index (%) (bile duct)	0.17 ± 0.05	0.18 ± 0.10	1.2 ± 0.4**	1.6 ± 0.5	2.2 ± 0.4*
TUNEL-labeling index (%) (hepatocyte)	0.23 ± 0.10	0.22 ± 0.48	0.38 ± 0.15	0.29 ± 0.09	0.36 ± 0.20
Aspertate aminotransferase (IU/L)	134 ± 9	149 ± 19	159 ± 37	158 ± 24	139 ± 11
Alanine aminotransferase (IU/L)	45 ± 2	41 ± 5	65 ± 5	63 ± 3	66 ± 4
Alkaline phosphatase (U/L)	1141 ± 199	994 ± 231	992 ± 146	921 ± 242	1067 ± 62
Total protein (g/dL)	6.2 ± 0.2	6.3 ± 0.2	6.5 ± 0.1	6.5 ± 0.2	6.4 ± 0.2
Albumin (g/dL)	3.1 ± 0.1	3.1 ± 0.2	2.9 ± 0.1	2.8 ± 0.1	2.9 ± 0.1
Blood urea nitrogen (mg/dL)	17 ± 1	19 ± 2	18 ± 1	20 ± 1	19 ± 1
Creatinine (mg/dL)	0.22 ± 0.02	0.19 ± 0.01	0.20 ± 0.02	0.23 ± 0.02	0.22 ± 0.02

ND, not determined. $n = 5$.
*$P < 0.05$; PCK-treated versus PCK-untreated.
**$P < 0.01$; PCK-untreated versus control untreated.

as evaluated using routine histological sections (Figure 3, D and E). In control rats, there were no apparent histological changes observed in the liver because of the treatment (Figure 3, A and B).

Histomorphometric analysis using whole liver tissue sections showed that the mean liver cyst indexes of the PCK rats without and with treatment (10 mg/kg) were 7.9 and 4.1%, respectively, and there was a significant difference observed between them. The administration of 2 mg/kg gefitinib had no significant effects on the cystic dilation of intrahepatic bile ducts of PCK rats. No significant morphological changes were observed in the control rats after treatment at any dosage. Serum levels of aspartate aminotransferase, alanine aminotransferase, alkaline phosphatase, total protein, and albumin were not significantly different among any groups (Table 1).

The proliferative activity of the BECs of PCK rats, assessed using the KI-67-LI, was significantly inhibited by the gefitinib treatment (10 mg/kg), and these inhibitory effects on the cell proliferative activity were accompanied by the increased rate of apoptosis of BECs of PCK rats (Table 1). Hepatocyte apoptosis was not significantly affected by the gefitinib treatment at any dosage in both the control and PCK rats.

Kidneys

In contrast with the mild inhibitory effects of gefitinib on the dilation of intrahepatic bile ducts of PCK rats, no beneficial effects were observed on renal cyst development because of the treatment (Figure 3, H–J). Histologically, PCK rats without treatment exhibited cystic dila-

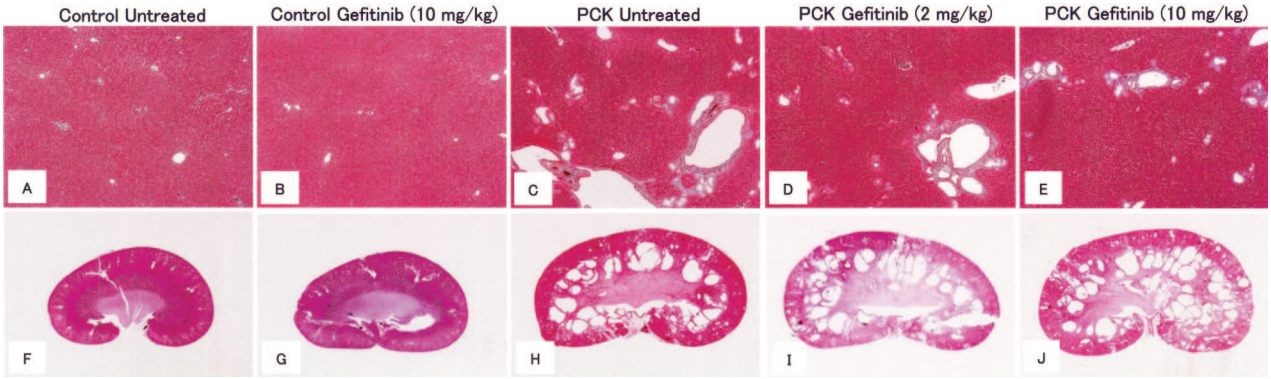

Figure 3. Effects of *in vivo* administration of gefitinib on the liver and kidney cyst pathology of the PCK rat. Control and PCK rats were treated with gefitinib or vehicle alone daily between 3 and 10 weeks of age. **A–E:** Representative liver sections stained with azan-Mallory. **F–J:** Representative kidney sections stained with H&E at the same magnification. Gefitinib improved cystic dilation of intrahepatic bile ducts of PCK rats, but no beneficial effects were observed on kidney lesions. Original magnifications, ×20 (**A–E**).

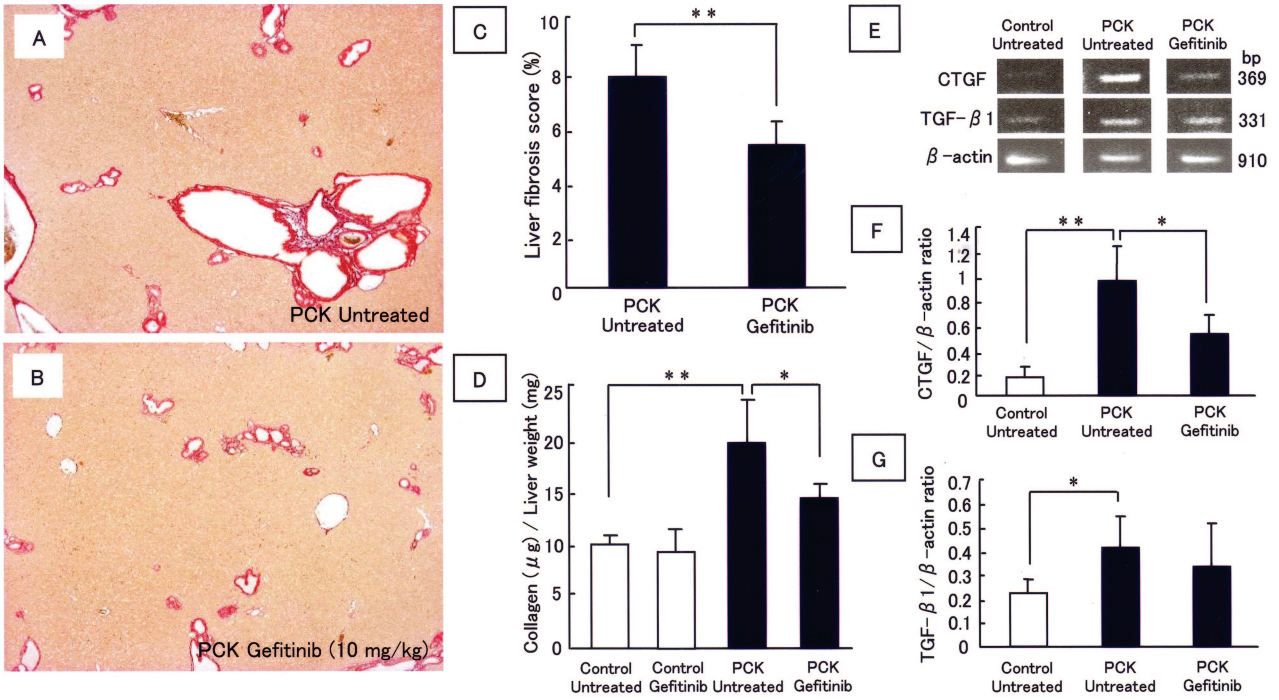

Figure 4. Inhibitory effects of gefitinib on liver fibrosis of the PCK rat. **A** and **B:** Representative photographs of the picrosirius red staining of the liver sections (**A:** PCK rats, untreated. **B:** PCK rats, treated with gefitinib, 10 mg/kg). **C:** Histological assessment of the liver fibrosis. The picrosirius red-stained area was determined in individual liver sections. **D:** Measurement of collagen content in the liver. Gefitinib (10 mg/kg) significantly reduced the collagen content in the livers of the PCK rats. **E:** RT-PCR analysis of CTGF and TGF-β1 mRNA expression in the whole liver. Results of semiquantitative analysis of the gel images are shown in **F** and **G**. Data represent the mean ± SD in four sets. $^{**}P < 0.01$. $^{*}P < 0.05$. Original magnifications, ×20.

tions of renal tubules at the corticomedullary junction and outer layer of the medulla (Figure 3H), and the cystic changes were not affected, or rather worsened, by the treatment (Figure 3, I and J). Histomorphometric analysis showed that the kidney cyst index was not significantly different between the PCK rats without and with the treatment, but the mean value was increased in PCK rats treated with gefitinib (10 mg/kg) (Table 1). The PCK rats without the treatment showed a significant increase in the kidney-to-body weight ratio compared with the normal rats, and the increase was not affected by the treatment (Table 1). The serum levels of blood urea nitrogen and creatinine were not significantly different among any of the groups (Table 1).

Effects of Gefitinib on Liver Fibrosis in Vivo

Histomorphometric analysis of liver fibrosis using the picrosirius red staining showed that the liver fibrosis of PCK rats was significantly improved by the administration of gefitinib (Figure 4, A–C). Measurement of the collagen content of the whole liver homogenates also showed that gefitinib significantly reduced collagen content in the livers of the PCK rats. In rats without the treatment, semiquantitative RT-PCR analysis showed that there was a significant increase in the expression of CTGF and TGF-β1 mRNA in the whole livers of the PCK rats compared with the control rats (Figure 4, E–G). Gefitinib significantly reduced the CTGF mRNA expression in the livers of PCK rats, whereas the expression of TGF-β1 mRNA was unaffected.

Three-Dimensional Observation of Intrahepatic Biliary Tree

Three-dimensional observation of the intrahepatic biliary tree using the silicon rubber cast study demonstrated that the intrahepatic biliary tree of the control rats showed fine branching and a reticular structure (Figure 5A), whereas the biliary tree of PCK rats without treatment showed multiple segmental and saccular dilatations, with the fine branching, as seen in the control rats, becoming unclear (Figure 5B). Treatment of the PCK rats with gefitinib (10 mg/kg) improved the multiple, segmental, and saccular dilatations of the intrahepatic bile ducts (Figure 5C), but the effects were incomplete.

EGFR Tyrosine Kinase Activity

The expression and activity of EGFR were measured with Western blot analysis using whole liver and kidney protein lysates. High levels of EGFR expression were detected similarly in the livers of the control and PCK rats without gefitinib treatment, and p-EGFR was also similarly detected in both rats (Figure 6A). The treatment of the PCK rats with gefitinib diminished the expression of p-EGFR in the liver (Figure 6A), confirming that the EGFR tyrosine kinase activity was inhibited by the treatment. In the kidney, the expression of EGFR was detected in the control and PCK rats without treatment to the same degree, but the expression levels were apparently weak compared with those of the liver (Figure 6B). The expres-

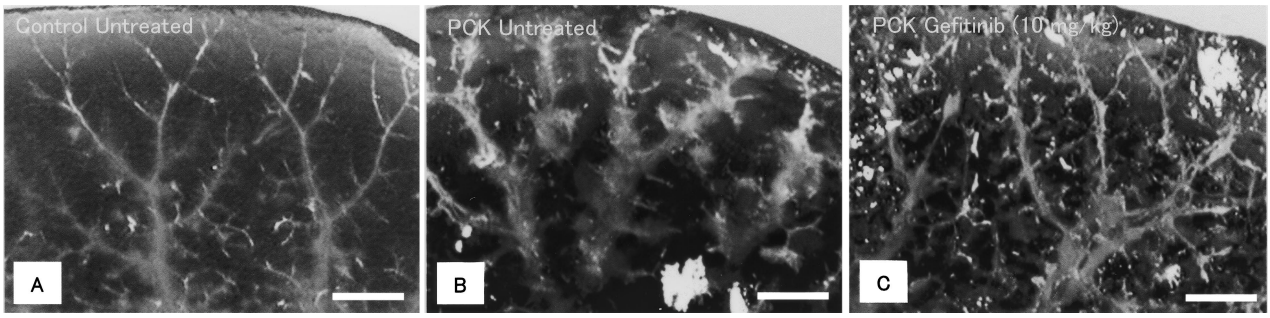

Figure 5. Three-dimensional observation of intrahepatic biliary tree. An intrahepatic biliary tree was constructed by the use of the silicon rubber cast study. **A:** Control rats, untreated. **B:** PCK rats, untreated. **C:** PCK rats, treated with gefitinib (10 mg/kg). Gefitinib inhibited the cystic dilation of intrahepatic bile ducts of PCK rats. Scale bars = 1 mm.

sion of p-EGFR in the untreated kidney was faint or invisible.

Expression of p-ERK1/2 and p-ERK5

As shown in Figure 6A, the whole liver of the PCK rat demonstrated the increased expression of p-ERK5 and contained no detectable amount of p-ERK1/2. The increased p-ERK5 expression in the PCK liver was reduced by the *in vivo* gefitinib treatment. Cultured BECs of PCK rats also showed the increased expression of p-ERK5, which was reduced by the gefitinib treatment *in vitro* (Figure 6C). In the kidney, the PCK rat showed the increased expression of p-ERK1/2 compared with the levels of the control rat without gefitinib treatment, but p-ERK1/2 expression in the kidney was not affected by gefitinib (Figure 6B). P-ERK5 was not detected in the kidneys of the control and PCK rats.

Localization of p-ERK1/2 and p-ERK5 in the liver and kidney was examined using immunohistochemistry. In the liver, no positive signals for p-ERK1/2 were detected in the interlobular bile ducts of the control rats (Figure 7A), whereas a few positive signals were observed in the nuclei of the biliary epithelium of the PCK rats without treatment (Figure 7B). Gefitinib reduced the number of p-ERK1/2-positive nuclei of the biliary epithelium of PCK rats, but a few p-ERK1/2-positive cells still remained visible after the treatment (Figure 7C, arrow). Positive signals for p-ERK5 were diffusely seen in the nuclei of the biliary epithelium and hepatocytes in both the control and PCK rats without treatment, and the signal intensity of biliary epithelium was remarkably higher in PCK rats (Figure 7, D and E). The reduction of the nuclear signal intensity for p-ERK5 was observed in the biliary epithelium of PCK rats after the treatment (Figure 7F).

In the kidney, the positive nuclear signals for p-ERK1/2 were observed in the renal tubules of the control rats (Figure 7G), and the collecting tubule-derived cyst epithelium of PCK rats without treatment diffusely expressed p-ERK1/2 (Figure 7H). The frequency and distribution of p-ERK1/2-positive cells in the kidneys of PCK rats were not significantly affected by the treatment (Figure 7I). There were no p-ERK5-positive signals observed in the kidney of both the control and PCK rats of any groups (Figure 7, J–L).

Discussion

Gefitinib is a tyrosine kinase inhibitor targeted to the ATP-binding domain of EGFR/HER1.[31,32] EGFR is expressed in a large proportion of epithelial tumors, and the

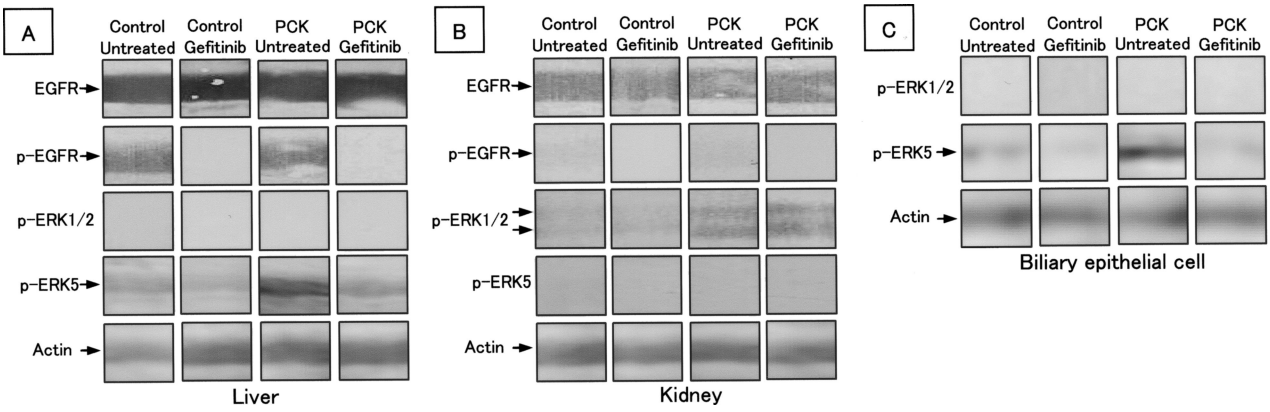

Figure 6. Western blot analysis of the expression of EGF receptor (EGFR), phosphorylated (p-)EGFR, p-ERK1/2, and p-ERK5. **A:** In the whole liver EGFR and p-EGFR expression were similarly detected in control and PCK rats without gefitinib treatment. Treatment with gefitinib (10 mg/kg) diminished p-EGFR expression in the liver. Expression of p-ERK5 was increased in the untreated PCK liver, which reduced after gefitinib treatment. **B:** In the kidney, expression levels of EGFR were weaker compared with those in the liver, and the expression of p-EGFR was faint or invisible, even in the untreated kidney. Increased expression of p-ERK1/2 was observed in untreated PCK kidney, and the expression was unchanged after gefitinib treatment. **C:** In cultured BECs, p-ERK5 was overexpressed in PCK rats, and the expression was reduced after gefitinib treatment. Data represent four independent experiments.

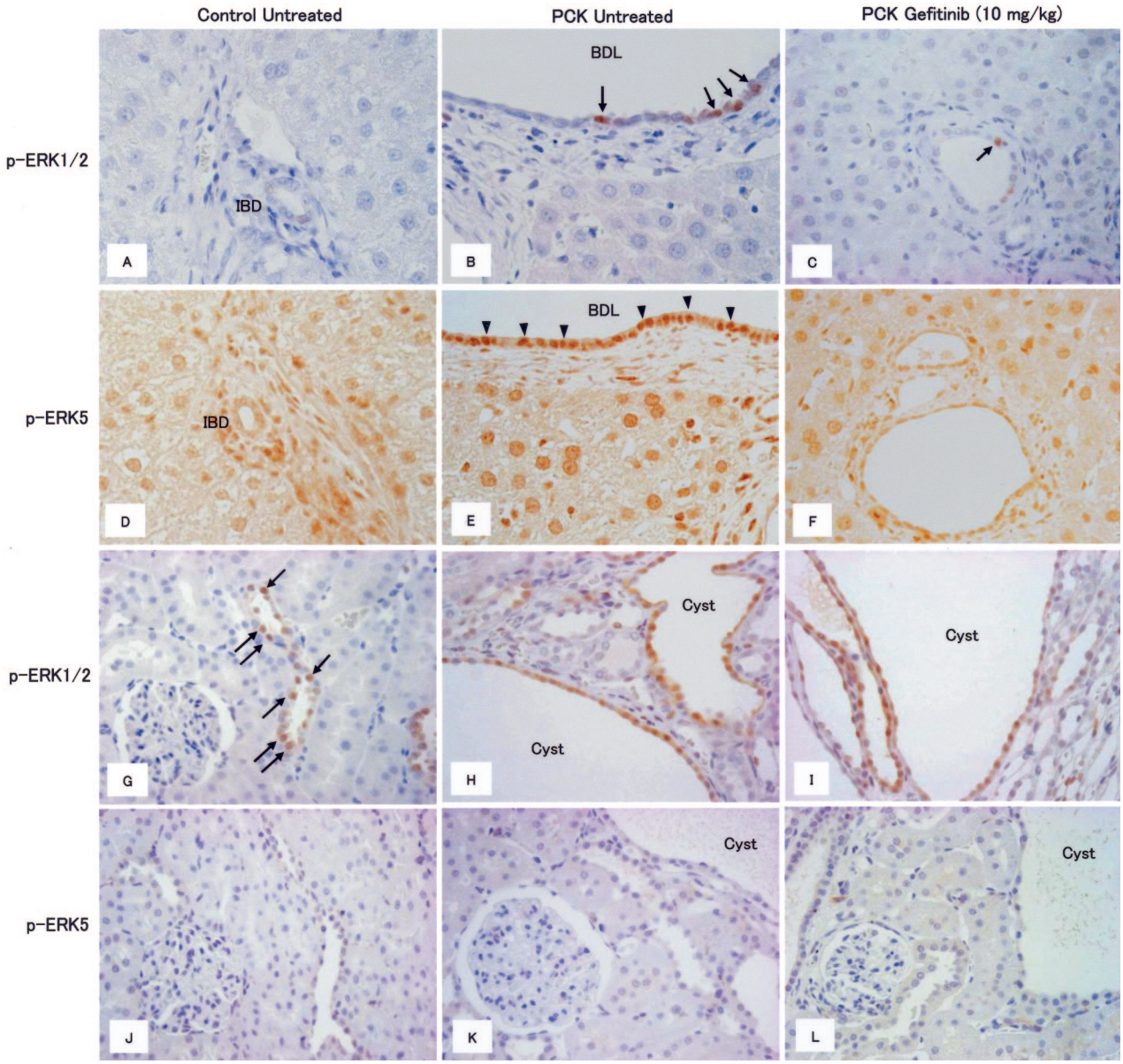

Figure 7. Immunohistochemical analysis of the expression of phosphorylated (p-)ERK1/2 and p-ERK5 in the liver (**A–F**) and kidney (**G–L**). A few positive signals of p-ERK1/2 were observed in nuclei of biliary epithelium of PCK rats without treatment (**B**, **arrows**). Gefitinib (10 mg/kg) reduced the number of p-ERK1/2-positive nuclei of biliary epithelium of PCK rats (**C**, **arrow**). Increased expression of p-ERK5 was observed in biliary epithelium of PCK rats without treatment (**E**, **arrowheads**), and gefitinib (10 mg/kg) reduced the signal intensity of p-ERK5 (**F**). Positive nuclear signals for p-ERK1/2 were observed in the renal tubules of the control rats (**G**, **arrows**), and collecting tubule-derived cyst epithelium of PCK rats without treatment showed diffuse positive staining (**H**). **I:** Gefitinib (10 mg/kg) had no effect on the frequency and distribution of p-ERK1/2-positive cells in the PCK kidney. There were no p-ERK5-positive signals in the kidney (**J–L**). IBD, interlobular bile duct; BDL, bile duct lumen. Original magnifications, ×400.

activation of EGFR triggers downstream signaling pathways, such as the Ras/Raf/ERK/MAPK and PI3K/Akt pathways, which regulate the cellular processes involved in tumor survival and growth. Gefitinib has been approved for the treatment of patients with epithelial tumors, particularly for non-small cell lung cancer. According to our previous study,[28] BECs of PCK rats diffusely expressed EGFR, and gefitinib strongly inhibited the abnormal growth of BECs of PCK rats *in vitro*. In this study, therefore, we aimed to inhibit PKD as well as the fibrocystic liver disease of the PCK rat by the use of this anti-cancer agent.

As expected, experiments using the three-dimensional cell culture system showed that gefitinib had inhibitory effects on cyst formation of BECs with reduced cell proliferative activity *in vitro*. Caroli's disease with congenital hepatic fibrosis is characterized by a congenital dilation of the intrahepatic bile ducts associated with portal fibrosis. The patient's age at onset of the initial symptoms of Caroli's disease has been reported to range from the neonatal period to 60 years of age.[33] From the therapeutic viewpoint, it would be important actually to inhibit the progression of the bile duct dilation into an advanced state, rather than to prevent cystic dilation of the bile ducts which are not yet dilated. Our *in vitro* experiments using the three-dimensional cell culture system showed that gefitinib could decrease the once formed biliary

cysts in size and number. In addition, the inhibitory effects were more prominent in the BECs of PCK rats than those of the control rats, consistent with our previous findings that the MEK5/ERK5 pathway was activated in the BECs of PCK rats.[28]

Apoptosis was induced more frequently in the BECs of PCK rats by the treatment. Blockage of the EGFR signaling pathways results in the retardation of cell-cycle progression and the induction of apoptosis in EGFR-expressing tumor cells. It has been suggested that the cell-cycle retardation is mediated by the up-regulation of cyclin-dependent kinase inhibitors p21 and p27.[34,35] The induction of apoptosis is mediated by a decrease in the expression level of an anti-apoptotic protein Bcl-2[36] or by the activation of a proapoptotic protein BAD.[37] In this study, we confirmed that gefitinib induced apoptosis in cultured nontumorous BECs, which was associated with the inhibition of biliary cyst formation.

In the absence of gefitinib, the basal apoptosis line level was not significantly different between the BECs of the control and PCK rats *in vitro*. *In vivo*, however, apoptosis occurred more frequently in the BECs of the PCK rats than in those of the control rats without gefitinib treatment. In the present study, an increased level of expression of TGF-β1 mRNA was observed in the whole livers of PCK rats. In addition, according to our previous study,[28] cultured BECs overexpressed TGF-β receptor type 1. Because TGF-β mediates apoptosis in various types of epithelial cells,[38] one possible explanation for the increased apoptosis rate of BECs in PCK rats without treatment *in vivo* may be attributable to the overexpression of TGF-β1 in the liver.

In vitro, apoptosis was induced more frequently in the BECs of the PCK rats than in the controls by the gefitinib treatment. Recent studies have demonstrated that the inhibition of ERK5 stimulates apoptosis in endothelial cells.[39] It has been reported that mek5 (−/−) embryos showed a marked decrease in proliferation and an increase in apoptosis in the heart, head, and dorsal regions of the mutant embryos.[40] Because MEK5 is overexpressed in the BECs of PCK rats,[28] they may have a more sustainable apoptotic response as well as growth inhibition by gefitinib through the inhibition of the MEK5/ERK5 cascade. It is also probable that the fact that apoptosis was markedly induced in the BECs of the PCK rats, rather than in the hepatocytes after gefitinib treatment, was attributable to the overexpression of MEK5 in the BECs.

Despite the strong inhibitory effects on biliary cyst formation of gefitinib *in vitro*, the administration of gefitinib to PCK rats resulted in incomplete inhibitory effects on the cystic dilation of the intrahepatic bile ducts. Recent studies showed that treatment of the PCK rat with EGFR tyrosine kinase inhibitors, EKI-785 and EKB-569, led to mild, but not significant, improvement in the liver cyst volume.[26]

In this study, p-EGFR was undetectable in the liver after gefitinib treatment, but immunostaining showed that p-ERK1/2 was persistently expressed in the BECs of PCK rats after treatment. Although a number of studies have implicated the importance of the EGF/TGF-α/EGFR pathway in the pathogenesis of PKD, the proliferation of cholangiocytes seems not to be simply mediated by this pathway. For example, the hepatocyte growth factor/met, TGF-β, and vascular endothelial growth factor induce cholangiocyte proliferation.[41] Receptors of vascular endothelial growth factor, Flk-1 and Flt-4, are expressed by cholangiocytes, and the stimulation of Flk-1 by vascular endothelial growth factor activates ERK1/2.[42] Moreover, recent studies have shown that liver cyst fluid of patients with ADPKD contained various mitogenic factors, including vascular endothelial growth factor.[43] These results indicate that the aberrant proliferation of BECs of PCK rats is not simply attributable to the activation of EGFR tyrosine kinase, and other factors may contribute to liver cyst pathogenesis *in vivo*.

Our data showed that the inhibition of the bile duct proliferation led to the improvement of liver fibrosis, and this effect was accompanied by the reduced expression of CTGF mRNA. CTGF can promote organ fibrosis, including the liver, by triggering fibroblast proliferation and up-regulating extracellular matrix production.[44] It has been shown that proliferating bile ducts are a major source of CTGF in rat biliary fibrosis.[45] In fact, our recent *in situ* hybridization studies showed that BECs of patients with congenital hepatic fibrosis expressed CTGF mRNA.[46] One possibility is that gefitinib reduced bile duct proliferation, which in turn led to the reduction of the local level of CTGF expression, and the improvement of liver fibrosis in PCK rats.

According to our previous study,[28] the BECs of PCK rats overexpressed mRNA for basic fibroblast growth factor. This suggests that the inhibition of the bile duct proliferation of PCK rats by gefitinib may lead to the reduction of the local basic fibroblast growth factor level, and the reduction may also relate to the improvement of liver fibrosis. In addition, despite the fact that gefitinib is often referred as a specific inhibitor of EGFR,[47] it has been reported that gefitinib inhibits the activity of other intracellular transmembrane tyrosine kinases, including that of the fibroblast growth factor receptor. Thus, the inhibition of the basic fibroblast growth factor signaling pathway may also contribute to the improvement of liver fibrosis.

No beneficial effect of gefitinib on kidney cystogenesis in this study is consistent with the low or faint expression of EGFR and p-EGFR in the kidney, as demonstrated by Western blot analysis. Immunohistochemically, the p-ERK1/2-positive cells in the kidneys of PCK rats were not significantly affected by the treatment, and there were no p-ERK5-positive signals observed in the kidneys of the PCK rats. These results indicate that the activation of EGFR tyrosine kinase is not involved in the kidney cyst development and progression of the PCK rat.

In the kidney, cAMP has a major role in renal cystogenesis, and the VPV2R is the major cAMP agonist.[48] Although cAMP inhibits the Ras-Raf-1-stimulated phosphorylation of ERK in normal kidney cells, it markedly increases the B-Raf kinase activity and ERK phosphorylation in polycystic kidney cells, including those in the PCK rat.[25] VPV2R and cAMP levels are elevated in the kidneys of PCK rats.[26] In addition, EGFR tyrosine kinase inhibition had no beneficial effect on the PKD of the PCK

rat in our experiments as well as in those reported by others.[26] Therefore, the expression of p-ERK1/2 in the kidney cyst lining epithelial cells of the PCK rat may be associated with the cAMP pathway, not with the EGF/TGF-α/EGFR pathway. Because the expression of VPV2R is absent in the liver, the mechanisms of cyst development and progression of the PCK rat may be different between the liver and kidney.

Therapeutic interventions have been applied to various animal models of PKD.[48] Among the reported therapies, the VPV2R antagonists OPC-31260 and OPC-41061 seem to be most effective and the only established therapy for kidney lesions of the PCK rat. However, neither of the VPV2R antagonists inhibited the development of fibrocystic liver disease.[23,25] Although we failed to complete the inhibition of the fibrocystic liver disease of the PCK rat in this study, further studies aimed at the inhibition of fibrocystic liver lesions of the PCK rat, a slowly progressive model of ARPKD, are still required because liver disease remains a major cause of mortality in elderly patients of ARPKD.

Acknowledgment

We thank AstraZeneca (Macclesfield, UK) for providing the gefitinib (Iressa).

References

1. Nakanuma Y, Terada T, Ohta G, Kurachi M, Matsubara F: Caroli's disease in congenital hepatic fibrosis and infantile polycystic disease. Liver 1982, 2:346–354
2. Sanzen T, Harada K, Yasoshima M, Kawamura Y, Ishibashi M, Nakanuma Y: Polycystic kidney rat is a novel animal model of Caroli's disease associated with congenital hepatic fibrosis. Am J Pathol 2001, 158:1605–1612
3. Wilson PD: Polycystic kidney disease. N Engl J Med 2004, 350:151–164
4. Harris PC, Rossetti S: Molecular genetics of autosomal recessive polycystic kidney disease. Mol Genet Metab 2004, 81:75–85
5. Ward CJ, Hogan MC, Rossetti S, Walker D, Sneddon T, Wang X, Kubly V, Cunningham JM, Bacallao R, Ishibashi M, Milliner DS, Torres VE, Harris PC: The gene mutated in autosomal recessive polycystic kidney disease encodes a large, receptor-like protein. Nat Genet 2002, 30:259–269
6. Onuchic LF, Furu L, Nagasawa Y, Hou X, Eggermann T, Ren Z, Bergmann C, Senderek J, Esquivel E, Zeltner R, Rudnik-Schoneborn S, Mrug M, Sweeney W, Avner ED, Zerres K, Guay-Woodford LM, Somlo S, Germino GG: PKHD1, the polycystic kidney and hepatic disease 1 gene, encodes a novel large protein containing multiple immunoglobulin-like plexin-transcription-factor domains and parallel beta-helix 1 repeats. Am J Hum Genet 2002, 70:1305–1317
7. Bergmann C, Senderek J, Kupper F, Schneider F, Dornia C, Windelen E, Eggermann T, Rudnik-Schoneborn S, Kirfel J, Furu L, Onuchic LF, Rossetti S, Harris PC, Somlo S, Guay-Woodford L, Germino GG, Moser M, Buttner R, Zerres K: PKHD1 mutations in autosomal recessive polycystic kidney disease (ARPKD). Hum Mutat 2004, 23:453–463
8. Zhang MZ, Mai W, Li C, Cho SY, Hao C, Moeckel G, Zhao R, Kim I, Wang J, Xiong H, Wang H, Sato Y, Wu Y, Nakanuma Y, Lilova M, Pei Y, Harris RC, Li S, Coffey RJ, Sun L, Wu D, Chen XZ, Breyer MD, Zhao ZJ, McKanna JA, Wu G: PKHD1 protein encoded by the gene for autosomal recessive polycystic kidney disease associates with basal bodies and primary cilia in renal epithelial cells. Proc Natl Acad Sci USA 2004, 101:2311–2316
9. Wang S, Luo Y, Wilson PD, Witman GB, Zhou J: The autosomal recessive polycystic kidney disease protein is localized to primary cilia, with concentration in the basal body area. J Am Soc Nephrol 2004, 15:592–602
10. Ward CJ, Yuan D, Masyuk TV, Wang X, Punyashthiti R, Whelan S, Bacallao R, Torra R, LaRusso NF, Torres VE, Harris PC: Cellular and subcellular localization of the ARPKD protein; fibrocystin is expressed on primary cilia. Hum Mol Genet 2003, 12:2703–2710
11. Masyuk TV, Huang BQ, Masyuk AI, Ritman EL, Torres VE, Wang X, Harris PC, Larusso NF: Biliary dysgenesis in the PCK rat, an orthologous model of autosomal recessive polycystic kidney disease. Am J Pathol 2004, 165:1719–1730
12. Masyuk TV, Huang BQ, Ward CJ, Masyuk AI, Yuan D, Splinter PL, Punyashthiti R, Ritman EL, Torres VE, Harris PC, LaRusso NF: Defects in cholangiocyte fibrocystin expression and ciliary structure in the PCK rat. Gastroenterology 2003, 125:1303–1310
13. Moser M, Matthiesen S, Kirfel J, Schorle H, Bergmann C, Senderek J, Rudnik-Schoneborn S, Zerres K, Buettner R: A mouse model for cystic biliary dysgenesis in autosomal recessive polycystic kidney disease (ARPKD). Hepatology 2005, 41:1113–1121
14. MacRae Dell K, Nemo R, Sweeney Jr WE, Avner ED: EGF-related growth factors in the pathogenesis of murine ARPKD. Kidney Int 2004, 65:2018–2029
15. Richards WG, Sweeney WE, Yoder BK, Wilkinson JE, Woychik RP, Avner ED: Epidermal growth factor receptor activity mediates renal cyst formation in polycystic kidney disease. J Clin Invest 1998, 101:935–939
16. Sweeney Jr WE, Avner ED: Functional activity of epidermal growth factor receptors in autosomal recessive polycystic kidney disease. Am J Physiol 1998, 275:F387–F394
17. Marfella-Scivittaro C, Quinones A, Orellana SA: cAMP-dependent protein kinase and proliferation differ in normal and polycystic kidney epithelia. Am J Physiol 2002, 282:C693–C707
18. Yamaguchi T, Pelling JC, Ramaswamy NT, Eppler JW, Wallace DP, Nagao S, Rome LA, Sullivan LP, Grantham JJ: cAMP stimulates the in vitro proliferation of renal cyst epithelial cells by activating the extracellular signal-regulated kinase pathway. Kidney Int 2000, 57:1460–1471
19. Hanaoka K, Guggino WB: cAMP regulates cell proliferation and cyst formation in autosomal polycystic kidney disease cells. J Am Soc Nephrol 2000, 11:1179–1187
20. Sweeney WE, Chen Y, Nakanishi K, Frost P, Avner ED: Treatment of polycystic kidney disease with a novel tyrosine kinase inhibitor. Kidney Int 2000, 57:339–340
21. Sweeney Jr WE, Hamahira K, Sweeney J, Garcia-Gatrell M, Frost P, Avner ED: Combination treatment of PKD utilizing dual inhibition of EGF-receptor activity and ligand bioavailability. Kidney Int 2003, 64:1310–1319
22. Torres VE, Sweeney Jr WE, Wang X, Qian Q, Harris PC, Frost P, Avner ED: EGF receptor tyrosine kinase inhibition attenuates the development of PKD in Han:SPRD rats. Kidney Int 2003, 64:1573–1579
23. Gattone II VH, Wang X, Harris PC, Torres VE: Inhibition of renal cystic disease development and progression by a vasopressin V2 receptor antagonist. Nat Med 2003, 9:1323–1326
24. Torres VE, Wang X, Qian Q, Somlo S, Harris PC, Gattone II VH: Effective treatment of an orthologous model of autosomal dominant polycystic kidney disease. Nat Med 2004, 10:363–364
25. Wang X, Gattone II V, Harris PC, Torres VE: Effectiveness of vasopressin V2 receptor antagonists OPC-31260 and OPC-41061 on polycystic kidney disease development in the PCK rat. J Am Soc Nephrol 2005, 16:846–851
26. Torres VE, Sweeney Jr WE, Wang X, Qian Q, Harris PC, Frost P, Avner ED: Epidermal growth factor receptor tyrosine kinase inhibition is not protective in PCK rats. Kidney Int 2004, 66:1766–1773
27. Wells A: EGF receptor. Int J Biochem Cell Biol 1999, 31:637–643
28. Sato Y, Harada K, Kizawa K, Sanzen T, Furubo S, Yasoshima M, Ozaki S, Ishibashi M, Nakanuma Y: Activation of the MEK5/ERK5 cascade is responsible for biliary dysgenesis in a rat model of Caroli's disease. Am J Pathol 2005, 166:49–60
29. Kawamura Y, Yoshida K, Nakanuma Y: Primary culture of rabbit gallbladder epithelial cells in collagen gel matrix. Lab Invest 1989, 61:350–356
30. Frankfurt OS, Krishan A: Identification of apoptotic cells by formamide-induced DNA denaturation in condensed chromatin. J Histochem Cytochem 2001, 49:369–378

31. Baselga J, Averbuch SD: ZD1839 ('Iressa') as an anticancer agent. Drugs 2000, 60(Suppl 1):32–41
32. Herbst RS, Fukuoka M, Baselga J: Gefitinib—a novel targeted approach to treating cancer. Nat Rev Cancer 2004, 4:956–965
33. Pinto RB, Lima JP, da Silveira TR, Scholl JG, de Mello ED, Silva G: Caroli's disease: report of 10 cases in children and adolescents in southern Brazil. J Pediatr Surg 1998, 33:1531–1535
34. Di Gennaro E, Barbarino M, Bruzzese F, De Lorenzo S, Caraglia M, Abbruzzese A, Avallone A, Comella P, Caponigro F, Pepe S, Budillon A: Critical role of both p27KIP1 and p21CIP1/WAF1 in the antiproliferative effect of ZD1839 ('Iressa'), an epidermal growth factor receptor tyrosine kinase inhibitor, in head and neck squamous carcinoma cells. J Cell Physiol 2003, 195:139–150
35. Okubo S, Kurebayashi J, Otsuki T, Yamamoto Y, Tanaka K, Sonoo H: Additive antitumour effect of the epidermal growth factor receptor tyrosine kinase inhibitor gefitinib (Iressa, ZD1839) and the antioestrogen fulvestrant (Faslodex, ICI 182,780) in breast cancer cells. Br J Cancer 2004, 90:236–244
36. Ciardiello F, Caputo R, Borriello G, Del Bufalo D, Biroccio A, Zupi G, Bianco AR, Tortora G: ZD1839 (IRESSA), an EGFR-selective tyrosine kinase inhibitor, enhances taxane activity in bcl-2 overexpressing, multidrug-resistant MCF-7 ADR human breast cancer cells. Int J Cancer 2002, 98:463–469
37. Gilmore AP, Valentijn AJ, Wang P, Ranger AM, Bundred N, O'Hare MJ, Wakeling A, Korsmeyer SJ, Streuli CH: Activation of BAD by therapeutic inhibition of epidermal growth factor receptor and transactivation by insulin-like growth factor receptor. J Biol Chem 2002, 277:27643–27650
38. Schuster N, Krieglstein K: Mechanisms of TGF-β-mediated apoptosis. Cell Tissue Res 2002, 307:1–14
39. Pi X, Yan C, Berk BC: Big mitogen-activated protein kinase (BMK1)/ERK5 protects endothelial cells from apoptosis. Circ Res 2004, 94:362–369
40. Wang X, Merritt AJ, Seyfried J, Guo C, Papadakis ES, Finegan KG, Kayahara M, Dixon J, Boot-Handford RP, Cartwright EJ, Mayer U, Tournier C: Targeted deletion of mek5 causes early embryonic death and defects in the extracellular signal-regulated kinase 5/myocyte enhancer factor 2 cell survival pathway. Mol Cel Biol 2005, 25:336–345
41. Alpini G, McGill JM, Larusso NF: The pathobiology of biliary epithelia. Hepatology 2002, 35:1256–1268
42. Bernatchez PN, Allen BG, Gelinas DS, Guillemette G, Sirois MG: Regulation of VEGF-induced endothelial cell PAF synthesis: role of p42/44 MAPK, p38 MAPK and PI3K pathways. Br J Pharmacol 2001, 134:1253–1262
43. Nichols MT, Gidey E, Matzakos T, Dahl R, Stiegmann G, Shah RJ, Grantham JJ, Fitz JG, Doctor RB: Secretion of cytokines and growth factors into autosomal dominant polycystic kidney disease liver cyst fluid. Hepatology 2004, 40:836–846
44. Paradis V, Dargere D, Vidaud M, De Gouville AC, Huet S, Martinez V, Gauthier JM, Ba N, Sobesky R, Ratziu V, Bedossa P: Expression of connective tissue growth factor in experimental rat and human liver fibrosis. Hepatology 1999, 30:968–976
45. Sedlaczek N, Jia JD, Bauer M, Herbst H, Ruehl M, Hahn EG, Schuppan D: Proliferating bile duct epithelial cells are a major source of connective tissue growth factor in rat biliary fibrosis. Am J Pathol 2001, 158:1239–1244
46. Ozaki S, Sato Y, Yasoshima M, Harada K, Nakanuma Y: Diffuse expression of heparan sulfate proteoglycan and connective tissue growth factor in fibrous septa with many mast cells relate to unresolving hepatic fibrosis of congenital hepatic fibrosis. Liver Int 2005, 25:817–828
47. Cohen MH, Williams GA, Sridhara R, Chen G, McGuinn Jr WD, Morse D, Abraham S, Rahman A, Liang C, Lostritto R, Baird A, Pazdur R: United States Food and Drug Administration Drug Approval summary: gefitinib (ZD1839; Iressa) tablets. Clin Cancer Res 2004, 10:1212–1218
48. Torres VE: Therapies to slow polycystic kidney disease. Nephron Exp Nephrol 2004, 98:e1–e7